



Published in final edited form as:

J Immunol. 2011 May 15; 186(10): 5638–5647. doi:10.4049/jimmunol.1003801.

Noncanonical K27-Linked Polyubiquitination of TIEG1 Regulates Foxp3 Expression and Tumor Growth

Dong-Jun Peng^{†,‡,*}, Minghui Zeng^{†,‡,*}, Ryuta Muromoto[§], Tadashi Matsuda[§], Kazuya Shimoda[¶], Malayannan Subramaniam^{||}, Thomas C. Spelsberg^{||}, Wei-Zen Wei^{†,‡,*}, and K. Venuprasad^{†,‡,*}

*Karmanos Cancer Institute, Detroit, MI 48201

†Department of Oncology, Wayne State University School of Medicine, Detroit, MI 48201

‡Department of Immunology and Microbiology, Wayne State University School of Medicine, Detroit, MI 48201

§Graduate School of Pharmaceutical Sciences, Hokkaido University, Sapporo 060-0812, Japan

¶Department of Gastroenterology and Hematology, University of Miyazaki, Kiyotake, Miyazaki 889-1692, Japan

||Mayo Clinic and Foundation, Rochester, MN 55905

Abstract

Earlier, we demonstrated the essential role of Kruppel-like transcription factor, TIEG1, in TGF- β -induced regulatory T cell (Treg) development. In this article, we demonstrate that IL-6, which promotes Th17 development, abrogated TIEG1 nuclear translocation and inhibited TGF- β -induced Treg development. Tyrosine kinase Tyk2-mediated phosphorylation of TIEG1 at Tyr179 promoted noncanonical K-27-linked polyubiquitination, which inhibited TIEG1 nuclear translocation. To test the role of TIEG1-regulated Treg/Th17 development in antitumor immunity, we analyzed TRAMP-C2 tumor growth in TIEG1^{-/-} mice. The defective Treg development and elevated Th17 response resulted in enhanced immune reactivity in the tumor and inhibition of TRAMP-C2 tumor growth in TIEG1^{-/-} mice. Thus, our results uncovered a novel regulatory mechanism that modulates Tregs and may regulate tumor progression.

Natural regulatory T cells (Tregs) develop from single-positive thymocytes during their maturation in the thymus and bear a diverse TCR repertoire against a broad range of self-Ags (1). In addition to thymus-derived natural Tregs, Foxp3⁺ Tregs are generated extrathymically by the conversion of naive CD4⁺ T cells by the action of TGF- β , known as induced regulatory T cells (iTregs) (2, 3). Because most tumor-associated Ags are aberrantly expressed self-Ags, Tregs play a critical role in suppressing antitumor immune response (4, 5). Furthermore, most malignant cells secrete large amounts of TGF- β (6–10), which was shown to convert effector T cells into tumor Ag-specific Tregs by inducing Foxp3 expression (6, 11–13). Such tumor-induced Tregs suppress the priming and effector functions of antitumor effector cells and form a broad self-amplifying immunosuppressive network (14). Therefore, overcoming TGF- β -induced expansion and de novo generation of

Copyright © 2011 by The American Association of Immunologists, Inc. All rights reserved.

Address correspondence and reprint requests to Dr. K. Venuprasad, Karmanos Cancer Institute, 110 East Warren Avenue, Mail Code PR04IM, Detroit, MI 48201. poojaryv@karmanos.org.

Disclosures

The authors have no financial conflicts of interest.

Tregs is critical for the design of effective immunotherapeutic strategies for successful cancer treatment.

Although TGF- β is a potent anti-inflammatory cytokine that induces Foxp3 expression and Treg differentiation, in the presence of the proinflammatory cytokines IL-6, IL-21, and IL-23, CD4⁺ T cells differentiate into Th17 cells that can promote antitumor immunity (15–19). The intracellular signaling pathways that link TGF- β signaling to these diverse, and even opposing, T cell functions remain largely unclear. Whether Ag-stimulated CD4⁺ T cells differentiate into Foxp3⁺ Tregs or Th17 cells depends upon the cytokine-regulated balance between Foxp3 and ROR γ t. STAT3 is a crucial component of IL-6-mediated regulation of Th17 cells (20). Beyond these observations, the downstream mechanisms are not known.

We previously reported that Itch-mediated monoubiquitination is essential for TIEG1 nuclear translocation and Foxp3 expression. Interestingly, Itch also targets TIEG1 for polyubiquitination in the transient overexpression system (21). However, the physiological relevance of TIEG1 polyubiquitination is not known. Ubiquitin contains seven lysine residues, and its linkage to a substrate generally occurs via K48 or K63. K48-linked polyubiquitin predominantly targets proteins for proteasomal degradation, whereas K63-linked poly- and monoubiquitination regulate subcellular localization, protein function, or protein–protein interactions (22, 23). E3 ligases often target the same substrates differently for mono- or polyubiquitination under different physiological conditions. Such a phenomenon was reported for p53 and PTEN ubiquitination by MDM2 and Nedd4, respectively (24–26). However, the molecular signals and precise mechanisms that determine mono- versus polyubiquitination are not completely understood. In this article, we demonstrate that TGF- β and IL-6 differentially promote mono- and polyubiquitination of TIEG1 and regulate Treg/Th17 differentiation. The impact of TIEG1 on tumor immunity was investigated in TIEG1^{-/-} mice. Growth of TRAMP-C2 tumor was reduced in TIEG1^{-/-} mice and was accompanied by reduced Foxp3⁺ Tregs and an elevated Th17 response, suggesting that TIEG1 deficiency tilted the balance from suppressive toward effector immunity.

Materials and Methods

Mice

TIEG1^{-/-} mice were described previously (27). Rag1^{-/-} mice were purchased from The Jackson Laboratory (Bar Harbor, ME); C57BL/6 mice were purchased from Charles River Laboratory. All mice were housed in microisolator cages in the barrier facility of Karmanos Cancer Institute. All experiments were performed in accordance with the guidelines of the Institutional Animal Care and Use Committee of Wayne State University. Tyk2^{-/-} mice were described previously (28) and were kept under specific pathogen-free conditions. All experiments were performed according to the guidelines of the Institutional Animal Care and Use Committee of Hokkaido University.

Reagents and Abs

Cytokines TGF- β 1 and IL-6 were purchased from PeproTech. The following Abs were used for immunoblotting and immunoprecipitation: anti-KLF10/TIEG1 (ab73537; Abcam), anti-phosphotyrosine (PY99; Santa Cruz), anti-His (GE Healthcare), rabbit anti-Tyk2 (C20; Santa Cruz), mouse anti-GST (B14; Santa Cruz), rabbit anti-hemagglutinin (HA) (Y-11; Santa Cruz), anti-c-Myc (9E10; Santa Cruz), anti-actin (AC-15; Sigma), anti-histone H3 (Biolegend), and anti-Xpress (Invitrogen). Ni⁺-NTA beads were purchased from Qiagen.

Isolation of CD4⁺CD25⁻ T cells

CD4⁺CD25⁻ T cells from mouse spleen and lymph node were isolated using the CD4⁺CD62L⁺ T Cell Isolation Kit (Miltenyi Biotec), according to manufacturer's protocol. T cells were cultured in RPMI 1640 medium supplemented with 10% FBS and stimulated with 2 μg/ml plate-bound anti-CD3 (eBioscience) and 2 μg/ml soluble anti-CD28 (Biolegend).

Flow cytometry

Surface and intracellular staining were performed using the Mouse Regulatory T Cell Staining Kit (88-8111; eBioscience), according to the manufacturer's protocol. Briefly, spleen and lymph node cells were suspended in Flow Staining Buffer with 0.5 μg anti-CD4-FITC and incubated at 4°C for 30 min. Cells were fixed, permeabilized, subjected to intracellular staining with anti-Foxp3-PE or negative control Abs by incubation at 4°C for 1 h, and analyzed by flow cytometry.

Quantitative RT-PCR

Total RNA was extracted using an RNeasy Mini kit (Qiagen), according to the manufacturer's instructions, and reverse transcribed into cDNA using a Verso cDNA Synthesis kit (Thermo Scientific). Real-time PCR was performed using a Mastercycler realplex system (Eppendorf) and Light-Cycler 480 SYBR Green I Master kit (Roche). The abundance of mRNA was normalized to that of actin mRNA. The following primers were used: *Foxp3* primers, 5'-CCCATCCCCAGGAGTCTTG-3' and 5'-ACCATGACTAGGGGCACTGTA-3'; actin primers, 5'-GAAATCGTGCCTGACATCAAAG-3' and 5'-TGTAGTTTCATGGATGCCACAG-3'; IFN-γ primers, 5'-GAACTGGCAAAGGATGGTGA-3' and 5'-TGTGGGTTGTTGACCTCAAAC-3'; and IL-17 primers, 5'-TTTAACTCCCTTGGCGCAAAA-3' and 5'-CTTTCCTCCGCATTGACAC-3'.

Plasmid construction and cell transfection

Mouse TIEG1 cDNA (Open Biosystem) was cloned into pEF4-His vector (Invitrogen) to generate plasmid-encoding His₆-Xpress-tagged TIEG1. The truncated TIEG1 was amplified by PCR and then cloned into EcoRI/XbaI sites of pEF4-His B vector (Invitrogen). The tyrosine residue mutants of TIEG1 were generated using a site-directed mutagenesis kit (Stratagene). pMT2T-Tyk2 and pMT2T-Tyk2/K930I (kinase-deficient mutant) were kindly provided by Dr. John J. Krolewski (University of California-Irvine). TIEG1 cDNA was cloned into the BamHI/EcoRI sites of pGEX-4T-2 vector to generate plasmid-encoding GST-TIEG1. Tyk2 and Tyk2/K930I were subcloned into the EcoRI site of pGEX-5X-3 vector (GE Amersham) to generate plasmids encoding GST-Tyk2 and GST-Tyk2/K930I. Myc-Itch plasmid was a kind gift from Dr. Francesca Bernassola (Department of Experimental Medicine and Biochemical Sciences, University of Rome). Flag-Tyk2- and Flag-Tyk2/K930I-encoding plasmids were constructed by subcloning the Tyk2 or Tyk2/K930I fragment into the EcoRI site of pCMV-Tag 2A vector. Plasmids encoding HA-tagged ubiquitin and ubiquitin lysine mutants were obtained from Addgene (29), with the exception of ubiquitin mutants of K6, K11, K27, K29, and K27R, which were generated using a site-directed mutagenesis kit. 293T cells were cultured in DMEM medium supplemented with 10% FBS, 100 U/ml penicillin, and 100 μg/ml streptomycin. Cell transfection was performed using Lipofectamine 2000 (Invitrogen), according to the manufacturer's instruction.

Immunoprecipitation and Western blotting

Cell lysates were prepared in Nonidet P-40 (NP-40) lysis buffer (150 mM NaCl, 50 mM Tris-Cl [pH 8] and 1% NP-40 with the addition of protease inhibitor mixture [Roche] and 1 mM vanadate). Cell lysates were incubated with 1–2 μg Ab at 4°C for ~3 h, followed by the addition of 25 μl protein A/G plus agarose (Santa Cruz Biotechnology) for an additional hour at 4°C. The immunoprecipitates were washed five times with NP-40 lysis buffer and analyzed by Western blotting with appropriate Abs. Briefly, proteins were electrophoresed by 10–12% denaturing polyacrylamide gels and transferred to polyvinylidene difluoride membrane (Millipore). The membranes were probed with primary Abs, washed, and incubated with appropriate HRP-conjugated secondary Abs. The membranes were visualized by an ECL reagent (Amersham Pharmacia Biotech). Membranes were stripped by incubation for 30 min at 65°C in stripping buffer and then reprobed with other Abs (21). In some experiments, cytoplasmic and nuclear fractions were prepared from total-cell lysates using Paris Protein and an RNA Isolation kit (Ambion).

Ubiquitination assay

Forty-eight hours after transfection with the indicated plasmids, 293T cells were treated with 10 μM proteasome inhibitor MG132 (Calbiochem) for 6 h, harvested, and lysed in NP-40 lysis buffer. His₆-TIEG1 was isolated by the Ni-NTA affinity-purification method, according to a published protocol (30). Briefly, cell lysates were diluted in 1 ml guanidine buffer (6 M guanidine-HCl, 0.1 M Na₂HPO₄/NaH₂PO₄ [pH 8]) with additions of 10 mM imidazole and 25 μl Ni-NTA agarose (Qiagen). The mixtures were incubated at 4°C for 3 h. The precipitated proteins were subsequently analyzed by immunoblotting with appropriate Abs.

GST pull-down assay

GST-TIEG1, GST-Tyk2, and GST-Tyk2/K930I fusion proteins were purified from BL21 (DE3) by Glutathione Sepharose beads (Amersham Pharmacia Biotech), according to the manufacturer's instructions. The purified GST, GST-TIEG1, GST-Tyk2, and GST-Tyk2/K930I proteins bound to Glutathione Sepharose beads were incubated with cell lysates at 4°C for 2–3 h, washed five times with PBS, and subjected to immunoblot analysis.

Retroviral construction and transduction

Flag-TIEG1 and Flag-TIEG1/Y179F cDNA amplified by PCR were cloned into retroviral vector MigR1. The retroviral particles were produced by Plat-E packaging cell line transiently transfected with retroviral constructs. Retroviral supernatants were collected 48 h after transfection. Naive CD4⁺ CD25⁻ T cells from TIEG1^{-/-} mice were stimulated with 2 $\mu\text{g}/\text{ml}$ anti-CD3 (eBioscience) and 2 $\mu\text{g}/\text{ml}$ soluble anti-CD28 (Biolegend) for 24 h and infected by adding 1:2 volume of retroviral supernatants supplemented with polybrene (6 $\mu\text{g}/\text{ml}$; Sigma), followed by centrifugation at 3000 rpm for 1 h at 32°C. Retroviral infection was repeated once at 24 h after the initial infection. T cells were maintained in complete RPMI 1640 medium with 100 U/ml rIL-2.

Conditioned medium

TRAMP-C2 cells were cultured in RPMI 1640 medium supplemented with 10% FBS, 5 $\mu\text{g}/\text{ml}$ insulin (I6634; Sigma), 100 U/ml penicillin, and 100 $\mu\text{g}/\text{ml}$ streptomycin. The conditioned medium (CM) was collected from 3-d culture of TRAMP-C2 cells and prepared by passing through a 0.45- μm filter. Isolated CD4⁺CD25⁻ T cells were incubated with T cells medium (RPMI 1640 supplemented with 10% FBS) or CM in the presence of 2 $\mu\text{g}/\text{ml}$ plate-bound anti-CD3 and soluble anti-CD28. T cells were collected and analyzed by quantitative PCR, as described above.

In vivo tumor growth

TRAMP-C2 cells were cultured in RPMI 1640 medium supplemented with 10% FBS, 5 $\mu\text{g}/\text{ml}$ insulin (I6634; Sigma), 100 U/ml penicillin, and 100 $\mu\text{g}/\text{ml}$ streptomycin. LLC cells were cultured in DMEM medium supplemented with 10% FBS, 100 U/ml penicillin, and 100 $\mu\text{g}/\text{ml}$ streptomycin. A total of $0.5\text{--}5 \times 10^6$ TRAMP-C2 cells or 1×10^6 LLC cells was injected s.c. into 8–12-wk-old male TIEG1^{-/-} mice or age-matched male C57BL/6 mice. Tumor growth was monitored thrice a week by measuring tumor length and width. The volume of the tumor was estimated by the formula $(\text{length} \times \text{width}^2)/2$.

Adoptive transfer of TIEG1^{-/-} T cells into Rag1^{-/-} mice

Naive CD4⁺CD25⁻ T cells (3×10^6) and CD8 T cells (1×10^6) isolated from TIEG1^{+/+} and TIEG1^{-/-} mice were adoptively transferred into Rag1^{-/-} mice by i.v. injection 3 d after TRAMP-C2 tumor cell inoculation. Tumor growth was monitored thrice a week.

Results

IL-6 negatively regulates TIEG1 nuclear translocation via Tyk2-mediated phosphorylation

Because TGF- β and IL-6 reciprocally regulate Treg and Th17 differentiation (16, 31–34), and TGF- β -induced TIEG1 nuclear translocation is essential for Foxp3 expression (21), we tested whether IL-6 negatively regulates TIEG1 to promote Th17 differentiation. Naive CD4⁺ T cells were stimulated with anti-CD3 + anti-CD28 in the presence of TGF- β alone or in combination with IL-6. To analyze the cellular distribution of TIEG1, we separated nuclear and cytoplasmic fractions and immunoblotted these fractions with anti-TIEG1 Ab. Consistent with our previous report (21), TGF- β treatment resulted in nuclear translocation of TIEG1; however, TIEG1 was predominantly located in the cytoplasm of the cells stimulated with IL-6 (Fig. 1A). This finding suggested that IL-6 inhibits nuclear localization of TIEG1 as a negative-regulatory mechanism to promote Th17. Because IL-6 stimulation induces tyrosine phosphorylation of several intracytoplasmic proteins, we tested whether TIEG1 is also tyrosine phosphorylated. As shown in Fig. 1B, TIEG1 was tyrosine phosphorylated in naive CD4⁺ T cells stimulated in the presence of TGF- β and IL-6 but not TGF- β alone, suggesting a critical role for phosphorylation-dependent cytoplasmic-to-nuclear shuttling of TIEG1 in Treg/Th17 differentiation.

Next, we sought to identify the upstream kinase that induced TIEG1 phosphorylation. Tyk2, a nonreceptor tyrosine kinase belonging to the Jak family, is activated when IL-6 binds to its receptors (35, 36). A Tyk2 mutation is associated with hyper-IgE syndrome (37), and T cells from hyper-IgE syndrome patients failed to differentiate into Th17 cells (38). Defective IL-17 expression was also reported in $\gamma\delta$ T cells from Tyk2^{-/-} mice (39). In addition, a natural mutation in the pseudokinase domain of Tyk2 accounted for increased susceptibility to infection and resistance to collagen-induced arthritis in B10.Q/J mice (40, 41). All of these suggest a possible link between the IL-6–Tyk2 pathway in Treg and Th17 differentiation. We hypothesized that, upon binding of IL-6 to its receptor, activated Tyk2 phosphorylates TIEG1. To test this hypothesis, we transiently transfected 293T cells with plasmids encoding wild-type (WT) Tyk2 or kinase-deficient mutant (K930I) Tyk2 and TIEG1. After 24 h, cells were treated with a phosphatase inhibitor (pervanadate) for 20 min. Cell extracts were immunoprecipitated with anti-His and immunoblotted with antiphosphotyrosine to analyze TIEG1 tyrosine phosphorylation. As shown in Fig. 1C, WT Tyk2 induced TIEG1 phosphorylation but not the kinase mutant. To further confirm the specificity of Tyk2 as the kinase, we stimulated naive CD4 T cells from Tyk2^{+/+} and Tyk2^{-/-} mice (28) with anti-CD3 and anti-CD28 in the presence of TGF- β alone or in combination with IL-6. TIEG1 was immunoprecipitated using anti-TIEG1 Ab and immunoblotted with anti-p-tyrosine Ab. As shown in Fig. 1D, stimulation of Tyk2^{+/+} CD4

T cells with IL-6 resulted in TIEG1 phosphorylation but not in Tyk2^{-/-} cells. These data strongly supported that Tyk2 phosphorylates TIEG1.

To understand the molecular mechanism underlying Tyk2-mediated TIEG1 tyrosine phosphorylation, we examined whether Tyk2 physically associates with TIEG1. TIEG1 was coimmunoprecipitated by anti-Tyk2 Ab, or vice versa, in transiently transfected 293T cells (Supplemental Fig. 1A). Further, we generated GST-TIEG1 and GST-Tyk2 fusion protein and performed pull-down assays. GST-TIEG1 precipitated Tyk2 from the cellular lysate of 293T cells transiently transfected with Tyk2; similarly, GST-Tyk2 precipitated TIEG1 (Supplemental Fig. 1B). To test whether the endogenously expressed TIEG1 and Tyk2 interact in naive CD4 T cells, we performed coimmunoprecipitation experiments using anti-TIEG1 and anti-Tyk2 Abs. As expected, anti-TIEG1 Ab coprecipitated Tyk2, and vice versa, in cells stimulated with IL-6 but not TGF- β alone (Fig. 1E).

TIEG1 phosphorylation at Y179 inhibits TIEG1 and Foxp3 expression

To identify the tyrosine residue that undergoes phosphorylation, we generated deletion mutants of TIEG1, as shown in Fig. 2A. Cotransfection with Tyk2 and the constructs encoding full-length TIEG1 or deletion mutants (1–220, and 1–370) resulted in TIEG1 phosphorylation but not deletion mutants 1–90, 1–160, 231–479, and 181–479 of TIEG1 (Fig. 2B). This result indicated that only tyrosine 179 is phosphorylated by Tyk2. To further confirm this result, we generated Y179F mutant TIEG1 (in which tyrosine 179 was mutated to phenylalanine). Cotransfection of TIEG1-Y179F with Tyk2 in 293T cells almost completely abolished phosphorylation (Fig. 2C). These results showed that Tyk2 phosphorylates TIEG1 at tyrosine 179. To understand the physiological relevance of these findings, we cloned TIEG1-Y179F mutant into MigR1-GFP retroviral vectors. We transduced TIEG1^{-/-} naive CD4⁺ CD25⁻ cells with WT or TIEG1-Y179F mutant by retroviral vectors, as we described previously (21). GFP⁺ cells were FACS sorted and stimulated under Treg (TGF- β)- and Th17 (TGF- β + IL-6)-inducing conditions. The nuclear and cytoplasmic fractions were separated, and TIEG1 localization was analyzed by immunoblotting. As shown in Fig. 3A, IL-6 inhibited nuclear translocation of WT TIEG1 but not TIEG1-Y179F mutant. Moreover, IL-6 failed to inhibit TGF- β -induced Foxp3 expression in TIEG1^{-/-} CD4⁺CD25⁻ cells reconstituted with TIEG1-Y179F mutants. Similarly, Y179F-transduced TIEG1^{-/-} T cells exhibited a marked defect in IL-17 expression (Fig. 3B). These data further highlight the phosphorylation-dependent negative regulation of TIEG1 in primary CD4 T cells during Treg/Th17 differentiation.

IL-6–Tyk2 pathway promotes K27-linked polyubiquitination of TIEG1

Previous studies suggested that phosphorylation can mark proteins for polyubiquitination (22, 42). To test whether Tyk2-mediated phosphorylation promoted TIEG1 polyubiquitination, we expressed His-TIEG1, HA-Ub, Myc-Itch, and Flag-Tyk2 in 293T cells. The ubiquitinated proteins were isolated using a Ni-NTA affinity purification method (30). As shown in Fig. 4A, coexpression of Tyk2 markedly enhanced Itch-mediated TIEG1 polyubiquitination. Further, increasing Tyk2 expression resulted in enhanced TIEG1 polyubiquitination (Fig. 4B), which suggested that Tyk2-mediated phosphorylation promotes TIEG1 polyubiquitination. Because IL-6 stimulation inhibited TIEG1 nuclear translocation, we wanted to know whether TIEG1 polyubiquitination is K48 or K63 linked. We coexpressed Myc-TIEG1, Flag-Tyk2, Itch, and HA-tagged mutants of Ub (Ub K48, in which all lysines, except K48, are mutated; UbK63, in which all lysines, except K63, are mutated) in 293T cells, and a ubiquitination assay was performed. Expression of WT Ub in the presence of Itch and Tyk2 readily induced TIEG1 polyubiquitination. To our surprise, neither UbK48 nor UbK63 catalyzed the ubiquitin chain on TIEG1 (Fig. 4C). Recent studies suggested that, in addition to conventional K48 and K63 polyubiquitination, other forms of

polyubiquitination are more common than originally thought (43–46). Therefore, we used UbK6, UbK11, UbK27, UbK29, and UbK33 to identify the topology of TIEG1 polyubiquitination. Interestingly, coexpression of UbK27 resulted in TIEG1 polyubiquitination. We consistently observed moderate polyubiquitination when UbK29 was coexpressed but not with UbK6, UbK11, UbK33, UbK48, or UbK63 (Fig. 4D). This suggested that Tyk2 promotes predominantly K27-linked polyubiquitination of TIEG1. To further confirm K27-linked polyubiquitination, we generated UbK27R (in which lysine residue at K27 of Ub was mutated to arginine). Coexpression of UbK27R with Itch, Tyk2, and TIEG1 resulted in markedly reduced TIEG1 polyubiquitination (Fig. 4E). To confirm that Tyk2-mediated phosphorylation is essential for K27-linked polyubiquitination, we coexpressed WT and Y179F mutant of TIEG1 (which is defective in phosphorylation) with Itch, Tyk2, and UbK27. As shown in Fig. 4F, there was a marked defect in the polyubiquitination of Y179F mutant compared with WT TIEG1. These results collectively suggested that Tyk2-mediated phosphorylation of TIEG1 promotes K27-linked polyubiquitination of TIEG1. Based on our results, we propose that when the naive CD4 T cells are stimulated in the presence of TGF- β , Itch targets TIEG1 for monoubiquitination. Monoubiquitinated TIEG1 translocates to the nucleus and binds to Foxp3 promoter to induce Foxp3 expression (21), whereas in the presence of IL-6, Tyk2 phosphorylates TIEG1, and Itch targets phosphorylated TIEG1 for polyubiquitination and prevent its nuclear translocation. This may divert Foxp3 transcription and promote Th17 differentiation (Supplemental Fig. 2).

Defective iTreg development and elevated Th17 response attenuate TRAMP-C2 tumor growth in TIEG1^{-/-} mice

Th17/Treg was shown to play a critical role in tumor immunity and immunotherapy (47). In hosts with large advanced tumors, Treg induction and expansion become dominant and result in poor effector T cell activation and tumor rejection (48–50). Phenotypic analysis of prostate-infiltrating lymphocytes revealed Th17/Treg skewing and an inverse correlation between Th17 cells and tumor progression (51). Moreover, vaccination with hsp70 induced IL-6 production in the prostate tissue, which triggered a Th17 response, resulting in rejection of established prostate tumors (52). All of these findings suggested an intimate connection between Treg/Th17 balance and immune surveillance. We previously demonstrated that TIEG1^{-/-} CD4⁺ T cells were resistant to TGF- β -mediated suppression and defective in Foxp3 expression upon TGF- β treatment in vitro (21). Another study reported enhanced IL-17 and IFN- γ production by TIEG1^{-/-} T cells (53). Therefore, we hypothesized that a reduced Treg and an elevated Th17 response in TIEG1^{-/-} mice will render enhanced antitumor immunity. This hypothesis was tested with prostate cancer TRAMP-C2 cells, which secrete large amounts of TGF- β . First, we tested whether TIEG1^{-/-} CD4⁺CD25⁻ cells are refractory to TRAMP-C2-derived TGF- β . Naive CD4⁺CD25⁻ cells from TIEG1^{+/+} and TIEG1^{-/-} mice were cultured with TRAMP-C2 CM. The cells were stimulated with anti-CD3 and anti-CD28 for 3–5 d (Fig. 5A). The effect of TRAMP-C2-derived TGF- β on the conversion of CD4⁺CD25⁻ cells into Foxp3⁺ cells was compared by real-time PCR, using the total RNA isolated from these cells. As expected, TIEG1^{+/+} cells expressed Foxp3, but the level of Foxp3 induction was markedly lower in TIEG1^{-/-} cells (Fig. 5B). To confirm that TGF- β derived from the TRAMP-C2 cells induced Foxp3 expression, we neutralized TGF- β in the supernatant using anti-TGF- β Ab. As expected, anti-TGF- β Ab inhibited Foxp3 expression in naive CD4 T cells, but the control isotype Ab did not (Fig. 5C). When IL-6 was added to TRAMP-C2 CM, TIEG1^{-/-} T cells produced significantly higher levels of IL-17 compared with TIEG1^{+/+} cells (Fig. 5D).

To test the impact of TIEG1 deficiency on tumor growth, we inoculated (0.5×10^6 – 5×10^6) TRAMP-C2 cells s.c. in the flanks of TIEG1^{+/+} and TIEG1^{-/-} mice. Tumor growth was

monitored thrice a week for 60 d. As shown in Fig. 6A, a majority of the TIEG1^{-/-} mice rejected TRAMP-C2 tumors; even when the tumors developed, their sizes were smaller (Fig. 6B). Because we demonstrated the essential role of TIEG1 in Treg development, we analyzed Foxp3⁺ Tregs in the spleen and draining lymph nodes of these mice by intracellular staining using anti-Foxp3 Ab. As shown in Fig. 6C and 6D, the percentage of CD4⁺Foxp3⁺ cells was markedly increased in the tumor-bearing TIEG1^{+/+} mice; however, in the TIEG1^{-/-} mice, the percentage of Tregs remained similar to that in the naive mice. Similarly, we noticed markedly reduced Foxp3 expression in the tumor mass collected from TIEG1^{-/-} mice compared with TIEG1^{+/+} mice. This suggested that the TIEG1 deficiency may affect the expansion and de novo generation of tumor-specific Tregs. Because tumor-specific Tregs actively suppress effector T cell responses, we tested whether defective Treg development in TIEG1^{-/-} mice correlated with elevated immune reactivity in the tumor. As expected, we found elevated levels of IFN- γ and IL-17 in the tumor-infiltrated cells in TIEG1^{-/-} mice (Fig. 6E) compared with TIEG1^{+/+} mice. Because we found elevated IL-17 in TIEG1^{-/-} tumors, we analyzed the expression of IL-6 transcripts in the RNA isolated from the whole tumor tissue. We detected IL-6 mRNA in the tumors from TIEG1^{+/+} and TIEG1^{-/-} mice (data not shown). This suggested that in the TRAMP-C2 tumor microenvironment there is an abundance of Treg-promoting TGF- β and Th17-promoting inflammatory IL-6. Because high levels of TGF- β produced by TRAMP-C2 cells induced Treg development and inhibited Th17 (54) in TIEG1^{+/+} tumor-bearing mice, Treg development may predominate, and TIEG1 deficiency may tilt the balance toward Th17 and antitumor immunity. To further test whether an enhanced antitumor immune response is unique to TRAMP-C2, we inoculated TIEG1^{+/+} and TIEG1^{-/-} mice with LLC cells. As shown in Supplemental Fig. 3, reduced LLC tumor growth was observed in TIEG1^{-/-} mice. These data collectively suggested that defective Foxp3 expression and elevated Th17 responses in TIEG1^{-/-} mice result in robust antitumor immune response and tumor rejection.

To confirm that TIEG1 deficiency regulates de novo generation of Tregs/Th17 cells in the tumor microenvironment, we set up an adoptive-transfer model. In this model, Rag1^{-/-} mice were injected with TRAMP-C2 cells, followed by infusion of CD25-depleted CD4 (3×10^6) and CD8 T cells (1×10^6) from naive TIEG1^{+/+} and TIEG1^{-/-} donors. In the WT environment, tumors grew progressively; however, tumor growth was markedly reduced and delayed in Rag1^{-/-} mice that received TIEG1^{-/-} T cells (Fig. 7A, 7B). Analysis of Foxp3 expression in tumor-infiltrating lymphocytes by intracellular staining revealed that a significant number of TIEG1^{+/+} donor CD4⁺CD25⁻ cells was converted into Foxp3⁺ cells. However, we detected only a few Foxp3⁺ cells in Rag1^{-/-} mice that received CD25-depleted TIEG1^{-/-} T cells (Fig. 7C). As expected, we also observed markedly increased numbers of IFN- γ ⁺ and IL-17⁺ cells in the Rag1^{-/-} mice that received TIEG1^{-/-} T cells (Fig. 7D). These results showed that iTregs generated in the tumor microenvironment played a significant role in the antitumor immune response.

Discussion

Although protein ubiquitination has been classically considered as a death signal, recent studies convincingly demonstrated that it also represents a means of protein modification, affecting protein-protein interaction, phosphorylation, and subcellular localization (55). K48-linked polyubiquitin chains are the principal signals for targeting substrates for degradation by the 26S proteasome, whereas K63-linked chains act in a range of processes, including protein trafficking, DNA repair, and inflammation. In addition, endogenous K6, K11, K27, K29, or K33-linked polyubiquitination of protein substrates has been reported; however, their function remains largely nebulous (44, 56). In this study, we demonstrated that Itch differentially targets TIEG1 for mono- and polyubiquitination and regulates its nuclear-to-cytoplasmic shuttling during Treg/Th17 differentiation. Interestingly, TIEG1

polyubiquitination was K27 linked, and whose function remains largely unknown. The E3 ligase TRAF6 was reported to promote K6, K27, and K29 ubiquitination of the Parkinson's disease proteins DJ-1 and α -synuclein, resulting in their accumulation in the cytoplasmic aggregates (57). K27-linked polyubiquitination was also shown to promote lysosomal localization of Jun (58). Our initial analysis revealed a bipartite nuclear localization signal (59–61) within the second zinc finger domain of TIEG1 (K. Venuprasad, unpublished observations), and K27-linked ubiquitination may block this nuclear localization signal. Another important observation of our study was that Tyk2, which is activated by IL-6, phosphorylates TIEG1 and acts as a recognition signal for K27-linked polyubiquitination. Previous studies showed that phosphorylation can create recognition-signal phosphodegrons for binding of an E3 ligase to the substrate (42, 62). Phosphorylation can also result in the exposure of degrons by inducing conformational change, although the phosphate itself does not directly contribute to recognition on the degraon. In addition, phosphorylation can regulate the access of an E3 ligase to its targets via phosphorylation-dependent transport of the substrate or the ligase between cellular compartments (42). It is not clear how TIEG1 phosphorylation results in K27-linked polyubiquitination, and it requires further detailed investigation.

Another important finding of our study was that inoculation of TRAMP-C2 cells into TIEG1^{-/-} mice resulted in tumor rejection. Also, reduced Foxp3⁺ Tregs and elevated IFN- γ and IL-17 by tumor-infiltrated cells suggested a robust immune reactivity against TRAMP-C2 cells in TIEG1^{-/-} mice. Again, our adoptive-transfer studies using Rag1^{-/-} mice clearly suggested that TIEG1^{-/-} T cells failed to convert into Foxp3⁺ Tregs, resulting in elevated Th17 responses and reduced tumor growth, which suggested a critical role for TIEG1 in immune surveillance. However, TIEG1 was shown to regulate transcription of TGF- β itself by binding to the consensus sequences on the TGF- β promoter (53). In addition to defective Treg development and elevated Th17 responses, TIEG1 may regulate additional mechanisms that contribute to the observed antitumor effects in TIEG1^{-/-} mice.

The expansion and de novo generation of tumor-specific Tregs has emerged as a major obstacle in successful immunotherapy against tumors (11). Especially in hosts bearing large advanced tumors, Treg induction and expansion become dominant, resulting in poor effector T cell activation and tumor rejection (48–50). For example, immunizing tumor-bearing mice with vaccine carrying a tumor Ag elicited tumor Ag-specific effector T cells and Tregs (48). Similarly, clinical investigations with human papilloma virus E6/E7 vaccines in cervical cancer patients provide further support for the concomitant induction of tumor-specific Tregs (50). Using the TRAMP-C2 prostate cancer cell line, which secretes high levels of TGF- β (7), it was demonstrated that tumor-secreted TGF- β converted the tumor Ag-specific T cells into Foxp3⁺ Tregs (6). Such Tregs inhibit the priming and effector function of antitumor effector cells and form a self-amplifying immune-suppressive network through its interaction with various APCs in the tumor microenvironment (14). Therefore, developing a vaccination strategy to increase the frequency of tumor-specific effector T cells, as well as to prevent Treg induction, is essential for successful treatment. Depleting Tregs using anti-CD25 Ab was demonstrated to enable the rejection of several types of transplantable tumors. Because Tregs are required for maintaining self-tolerance, prolonged, global, and nonspecific depletion of Tregs may breach self-tolerance (11, 63). Therefore, strategies are needed to selectively block the development of Tregs in the tumor site. It will be advantageous to eliminate suppressors while redirecting the precursor T cells to differentiate into effector cells, such as Th1 or Th17 cells (23). We describe a phosphorylation-dependent regulation of Treg/Th17 development by TIEG1. TIEG1 deficiency resulted in elevated IL-17 expression and reduced TRAMP-C2 tumor growth. Because higher levels of TGF- β promote the development of Tregs and suppress IL-6-mediated Th17 cell differentiation (54, 64, 65), it is likely that, in the absence of TIEG1, the effect of high concentrations of

TGF- β in the tumor microenvironment is nullified, resulting in elevated IL-17 expression. The role of IL-17 in tumor immunopathology has been controversial. Overexpression of IL-17 in some tumor cell lines promotes angiogenesis and tumor growth, suggesting a protumor activity (66). However, transgenic T cells polarized to a Th17 phenotype by treatment with TGF- β and IL-6 were shown to eradicate tumors (17–19). A significant inverse correlation between Th17 and tumor progression was reported in patients with prostate cancer (51). Therefore, Th17 cells provide protection against tumors in certain cases, as we observed in TIEG1-deficient mice. A better understanding of the molecular regulation of Treg/Th17 conversion could help to improve cancer immunotherapy strategies.

Supplementary Material

Refer to Web version on PubMed Central for supplementary material.

Acknowledgments

We thank Dr. Mohamed Oukka and Dr. Yi-Chi M. Kong for critical reading of the manuscript, Dr. Indrajit Sinha and Dr. Lisa Polin for help with experiments, Joyce Rees for technical assistance, and Dr. Marie Piechocki and Dr. Anagh Sahasrabudhe for helpful discussions.

This work was supported by National Cancer Institute Grants 1RC1CA146576-01 (to K.V.) and 2R01CA076340-11A2 and Department of Defense Grant W81XWH-10-1-0466 (to W.Z.W. and K.V.).

Abbreviations used in this article

CM	conditioned medium
HA	hemagglutinin
iTreg	induced regulatory T cell
NP-40	Nonidet P-40
Treg	regulatory T cell
WT	wild-type

References

1. Sakaguchi S, Powrie F. Emerging challenges in regulatory T cell function and biology. *Science*. 2007; 317:627–629. [PubMed: 17673654]
2. Chen W, Jin W, Hardegen N, Lei KJ, Li L, Marinos N, McGrady G, Wahl SM. Conversion of peripheral CD4⁺CD25⁻ naive T cells to CD4⁺ CD25⁺ regulatory T cells by TGF-beta induction of transcription factor Foxp3. *J. Exp. Med.* 2003; 198:1875–1886. [PubMed: 14676299]
3. Li MO, Flavell RA. TGF-beta: a master of all T cell trades. *Cell*. 2008; 134:392–404. [PubMed: 18692464]
4. Nishikawa H, Kato T, Tawara I, Saito K, Ikeda H, Kuribayashi K, Allen PM, Schreiber RD, Sakaguchi S, Old LJ, Shiku H. Definition of target antigens for naturally occurring CD4⁽⁺⁾ CD25⁽⁺⁾ regulatory T cells. *J. Exp. Med.* 2005; 201:681–686. [PubMed: 15753203]
5. Nishikawa H, Kato T, Tanida K, Hiasa A, Tawara I, Ikeda H, Ikarashi Y, Wakasugi H, Kronenberg M, Nakayama T, et al. CD4⁺ CD25⁺ T cells responding to serologically defined autoantigens suppress antitumor immune responses. *Proc. Natl. Acad. Sci. USA*. 2003; 100:10902–10906. [PubMed: 12947044]
6. Liu VC, Wong LY, Jang T, Shah AH, Park I, Yang X, Zhang Q, Lonning S, Teicher BA, Lee C. Tumor evasion of the immune system by converting CD4⁺CD25⁻ T cells into CD4⁺CD25⁺ T regulatory cells: role of tumor-derived TGF-beta. *J. Immunol.* 2007; 178:2883–2892. [PubMed: 17312132]

7. Zhang Q, Yang X, Pins M, Javonovic B, Kuzel T, Kim SJ, Parijs LV, Greenberg NM, Liu V, Guo Y, Lee C. Adoptive transfer of tumor-reactive transforming growth factor-beta-insensitive CD8+ T cells: eradication of autologous mouse prostate cancer. *Cancer Res.* 2005; 65:1761–1769. [PubMed: 15753372]
8. Shah AH, Lee C. TGF-beta-based immunotherapy for cancer: breaching the tumor firewall. *Prostate.* 2000; 45:167–172. [PubMed: 11027416]
9. Teicher BA. Malignant cells, directors of the malignant process: role of transforming growth factor-beta. *Cancer Metastasis Rev.* 2001; 20:133–143. [PubMed: 11831642]
10. Massagué J. TGFbeta in Cancer. *Cell.* 2008; 134:215–230. [PubMed: 18662538]
11. Colombo MP, Piconese S. Regulatory-T-cell inhibition versus depletion: the right choice in cancer immunotherapy. *Nat. Rev. Cancer.* 2007; 7:880–887. [PubMed: 17957190]
12. Valzasina B, Piconese S, Guiducci C, Colombo MP. Tumor-induced expansion of regulatory T cells by conversion of CD4+CD25– lymphocytes is thymus and proliferation independent. *Cancer Res.* 2006; 66:4488–4495. [PubMed: 16618776]
13. Yang ZZ, Novak AJ, Ziesmer SC, Witzig TE, Ansell SM. CD70+ non-Hodgkin lymphoma B cells induce Foxp3 expression and regulatory function in intratumoral CD4+CD25 T cells. *Blood.* 2007; 110:2537–2544. [PubMed: 17615291]
14. Qin FX. Dynamic behavior and function of Foxp3+ regulatory T cells in tumor bearing host. *Cell. Mol. Immunol.* 2009; 6:3–13. [PubMed: 19254475]
15. Littman DR, Rudensky AY. Th17 and regulatory T cells in mediating and restraining inflammation. *Cell.* 2010; 140:845–858. [PubMed: 20303875]
16. Dong C. TH17 cells in development: an updated view of their molecular identity and genetic programming. *Nat. Rev. Immunol.* 2008; 8:337–348. [PubMed: 18408735]
17. Martin-Orozco N, Muranski P, Chung Y, Yang XO, Yamazaki T, Lu S, Hwu P, Restifo NP, Overwijk WW, Dong C. T helper 17 cells promote cytotoxic T cell activation in tumor immunity. *Immunity.* 2009; 31:787–798. [PubMed: 19879162]
18. Muranski P, Boni A, Antony PA, Cassard L, Irvine KR, Kaiser A, Paulos CM, Palmer DC, Touloukian CE, Ptak K, et al. Tumor-specific Th17-polarized cells eradicate large established melanoma. *Blood.* 2008; 112:362–373. [PubMed: 18354038]
19. Hinrichs CS, Kaiser A, Paulos CM, Cassard L, Sanchez-Perez L, Heemskerk B, Wrzesinski C, Borman ZA, Muranski P, Restifo NP. Type 17 CD8+ T cells display enhanced antitumor immunity. *Blood.* 2009; 114:596–599. [PubMed: 19471017]
20. Yang XO, Panopoulos AD, Nurieva R, Chang SH, Wang D, Watowich SS, Dong C. STAT3 regulates cytokine-mediated generation of inflammatory helper T cells. *J. Biol. Chem.* 2007; 282:9358–9363. [PubMed: 17277312]
21. Venuprasad K, Huang H, Harada Y, Elly C, Subramaniam M, Spelsberg T, Su J, Liu YC. The E3 ubiquitin ligase Itch regulates expression of transcription factor Foxp3 and airway inflammation by enhancing the function of transcription factor TIEG1. *Nat. Immunol.* 2008; 9:245–253. [PubMed: 18278048]
22. Gao M, Karin M. Regulating the regulators: control of protein ubiquitination and ubiquitin-like modifications by extracellular stimuli. *Mol. Cell.* 2005; 19:581–593. [PubMed: 16137616]
23. Venuprasad K. Cbl-b and itch: key regulators of peripheral T-cell tolerance. *Cancer Res.* 2010; 70:3009–3012. [PubMed: 20395198]
24. Li M, Brooks CL, Wu-Baer F, Chen D, Baer R, Gu W. Mono-versus polyubiquitination: differential control of p53 fate by Mdm2. *Science.* 2003; 302:1972–1975. [PubMed: 14671306]
25. Trotman LC, Wang X, Alimonti A, Chen Z, Teruya-Feldstein J, Yang H, Pavletich NP, Carver BS, Cordon-Cardo C, Erdjument-Bromage H, et al. Ubiquitination regulates PTEN nuclear import and tumor suppression. *Cell.* 2007; 128:141–156. [PubMed: 17218261]
26. Wang X, Trotman LC, Koppie T, Alimonti A, Chen Z, Gao Z, Wang J, Erdjument-Bromage H, Tempst P, Cordon-Cardo C, et al. NEDD4-1 is a proto-oncogenic ubiquitin ligase for PTEN. *Cell.* 2007; 128:129–139. [PubMed: 17218260]
27. Subramaniam M, Gorny G, Johnsen SA, Monroe DG, Evans GL, Fraser DG, Rickard DJ, Rasmussen K, van Deursen JM, Turner RT, et al. TIEG1 null mouse-derived osteoblasts are

- defective in mineralization and in support of osteoclast differentiation in vitro. *Mol. Cell. Biol.* 2005; 25:1191–1199. [PubMed: 15657444]
28. Shimoda K, Kato K, Aoki K, Matsuda T, Miyamoto A, Shibamori M, Yamashita M, Numata A, Takase K, Kobayashi S, et al. Tyk2 plays a restricted role in IFN alpha signaling, although it is required for IL-12-mediated T cell function. *Immunity.* 2000; 13:561–571. [PubMed: 11070174]
 29. Lim KL, Chew KC, Tan JM, Wang C, Chung KK, Zhang Y, Tanaka Y, Smith W, Engelender S, Ross CA, et al. Parkin mediates nonclassical, proteasomal-independent ubiquitination of synphilin-1: implications for Lewy body formation. *J. Neurosci.* 2005; 25:2002–2009. [PubMed: 15728840]
 30. Treier M, Staszewski LM, Bohmann D. Ubiquitin-dependent c-Jun degradation in vivo is mediated by the delta domain. *Cell.* 1994; 78:787–798. [PubMed: 8087846]
 31. Bettelli E, Carrier Y, Gao W, Korn T, Strom TB, Oukka M, Weiner HL, Kuchroo VK. Reciprocal developmental pathways for the generation of pathogenic effector TH17 and regulatory T cells. *Nature.* 2006; 441:235–238. [PubMed: 16648838]
 32. Yang XO, Nurieva R, Martinez GJ, Kang HS, Chung Y, Pappu BP, Shah B, Chang SH, Schluns KS, Watowich SS, et al. Molecular antagonism and plasticity of regulatory and inflammatory T cell programs. *Immunity.* 2008; 29:44–56. [PubMed: 18585065]
 33. Korn T, Mitsdoerffer M, Croxford AL, Awasthi A, Dardalhon VA, Galileos G, Vollmar P, Stritesky GL, Kaplan MH, Waisman A, et al. IL-6 controls Th17 immunity in vivo by inhibiting the conversion of conventional T cells into Foxp3+ regulatory T cells. *Proc. Natl. Acad. Sci. USA.* 2008; 105:18460–18465. [PubMed: 19015529]
 34. Korn T, Reddy J, Gao W, Bettelli E, Awasthi A, Petersen TR, Bäckström BT, Sobel RA, Wucherpfennig KW, Strom TB, et al. Myelin-specific regulatory T cells accumulate in the CNS but fail to control autoimmune inflammation. *Nat. Med.* 2007; 13:423–431. [PubMed: 17384649]
 35. Leonard WJ, O'Shea JJ. Jaks and STATs: biological implications. *Annu. Rev. Immunol.* 1998; 16:293–322. [PubMed: 9597132]
 36. French JD, Walters DK, Jelinek DF. Transactivation of gp130 in myeloma cells. *J. Immunol.* 2003; 170:3717–3723. [PubMed: 12646637]
 37. Minegishi Y, Saito M, Morio T, Watanabe K, Agematsu K, Tsuchiya S, Takada H, Hara T, Kawamura N, Ariga T, et al. Human tyrosine kinase 2 deficiency reveals its requisite roles in multiple cytokine signals involved in innate and acquired immunity. *Immunity.* 2006; 25:745–755. [PubMed: 17088085]
 38. Milner JD, Brenchley JM, Laurence A, Freeman AF, Hill BJ, Elias KM, Kanno Y, Spalding C, Elloumi HZ, Paulson ML, et al. Impaired T(H)17 cell differentiation in subjects with autosomal dominant hyper-IgE syndrome. *Nature.* 2008; 452:773–776. [PubMed: 18337720]
 39. Nakamura R, Shibata K, Yamada H, Shimoda K, Nakayama K, Yoshikai Y. Tyk2-signaling plays an important role in host defense against *Escherichia coli* through IL-23-induced IL-17 production by gammadelta T cells. *J. Immunol.* 2008; 181:2071–2075. [PubMed: 18641345]
 40. Shaw MH, Boyartchuk V, Wong S, Karaghiosoff M, Ragimbeau J, Pellegrini S, Muller M, Dietrich WF, Yap GS. A natural mutation in the Tyk2 pseudokinase domain underlies altered susceptibility of B10.Q/J mice to infection and autoimmunity. *Proc. Natl. Acad. Sci. USA.* 2003; 100:11594–11599. [PubMed: 14500783]
 41. Ortmann R, Smeltz R, Yap G, Sher A, Shevach EM. A heritable defect in IL-12 signaling in B10.Q/J mice. I. In vitro analysis. *J. Immunol.* 2001; 166:5712–5719. [PubMed: 11313413]
 42. Hunter T. The age of crosstalk: phosphorylation, ubiquitination, and beyond. *Mol. Cell.* 2007; 28:730–738. [PubMed: 18082598]
 43. Ben-Saadon R, Zaaroor D, Ziv T, Ciechanover A. The polycomb protein Ring1B generates self atypical mixed ubiquitin chains required for its in vitro histone H2A ligase activity. *Mol. Cell.* 2006; 24:701–711. [PubMed: 17157253]
 44. Xu P, Duong DM, Seyfried NT, Cheng D, Xie Y, Robert J, Rush J, Hochstrasser M, Finley D, Peng J. Quantitative proteomics reveals the function of unconventional ubiquitin chains in proteasomal degradation. *Cell.* 2009; 137:133–145. [PubMed: 19345192]
 45. Wang H, Matsuzawa A, Brown SA, Zhou J, Guy CS, Tseng PH, Forbes K, Nicholson TP, Sheppard PW, Häcker H, et al. Analysis of nondegradative protein ubiquitylation with a

- monoclonal antibody specific for lysine-63-linked polyubiquitin. *Proc. Natl. Acad. Sci. USA*. 2008; 105:20197–20202. [PubMed: 19091944]
46. Huang H, Jeon MS, Liao L, Yang C, Elly C, Yates JR III, Liu YC. K33-linked polyubiquitination of T cell receptor-zeta regulates proteolysis-independent T cell signaling. *Immunity*. 2010; 33:60–70. [PubMed: 20637659]
 47. Zou W, Restifo NP. T(H)17 cells in tumour immunity and immunotherapy. *Nat. Rev. Immunol*. 2010; 10:248–256. [PubMed: 20336152]
 48. Zhou G, Drake CG, Levitsky HI. Amplification of tumor-specific regulatory T cells following therapeutic cancer vaccines. *Blood*. 2006; 107:628–636. [PubMed: 16179369]
 49. Melief CJ. Cancer immunotherapy by dendritic cells. *Immunity*. 2008; 29:372–383. [PubMed: 18799145]
 50. Welters MJ, Kenter GG, Piersma SJ, Vloon AP, Löwik MJ, Berends-van der Meer DM, Drijfhout JW, Valentijn AR, Wafelman AR, Oostendorp J, et al. Induction of tumor-specific CD4+ and CD8+ T-cell immunity in cervical cancer patients by a human papillomavirus type 16 E6 and E7 long peptides vaccine. *Clin. Cancer Res*. 2008; 14:178–187. [PubMed: 18172269]
 51. Sfanos KS, Bruno TC, Maris CH, Xu L, Thoburn CJ, DeMarzo AM, Meeker AK, Isaacs WB, Drake CG. Phenotypic analysis of prostate-infiltrating lymphocytes reveals TH17 and Treg skewing. *Clin. Cancer Res*. 2008; 14:3254–3261. [PubMed: 18519750]
 52. Kottke T, Sanchez-Perez L, Diaz RM, Thompson J, Chong H, Harrington K, Calderwood SK, Pulido J, Georgopoulos N, Selby P, et al. Induction of hsp70-mediated Th17 autoimmunity can be exploited as immunotherapy for metastatic prostate cancer. *Cancer Res*. 2007; 67:11970–11979. [PubMed: 18089828]
 53. Cao Z, Wara AK, Icli B, Sun X, Packard RR, Esen F, Stapleton CJ, Subramaniam M, Kretschmer K, Apostolou I, et al. Kruppel-like factor KLF10 targets transforming growth factor-beta1 to regulate CD4(+)/CD25(-) T cells and T regulatory cells. *J. Biol. Chem*. 2009; 284:24914–24924. [PubMed: 19602726]
 54. Zhou L, Lopes JE, Chong MM, Ivanov II, Min R, Victora GD, Shen Y, Du J, Rubtsov YP, Rudensky AY, et al. TGF-beta-induced Foxp3 inhibits T(H)17 cell differentiation by antagonizing RORgammat function. *Nature*. 2008; 453:236–240. [PubMed: 18368049]
 55. Mukhopadhyay D, Riezman H. Proteasome-independent functions of ubiquitin in endocytosis and signaling. *Science*. 2007; 315:201–205. [PubMed: 17218518]
 56. Malynn BA, Ma A. Ubiquitin makes its mark on immune regulation. *Immunity*. 2010; 33:843–852. [PubMed: 21168777]
 57. Zucchelli S, Codrich M, Marcuzzi F, Pinto M, Vilotti S, Biagioli M, Ferrer I, Gustincich S. TRAF6 promotes atypical ubiquitination of mutant DJ-1 and alpha-synuclein and is localized to Lewy bodies in sporadic Parkinson's disease brains. *Hum. Mol. Genet*. 2010; 19:3759–3770. [PubMed: 20634198]
 58. Ikeda H, Kerppola TK. Lysosomal localization of ubiquitinated Jun requires multiple determinants in a lysine-27-linked polyubiquitin conjugate. *Mol. Biol. Cell*. 2008; 19:4588–4601. [PubMed: 18716056]
 59. Taniguchi E, Toyoshima-Morimoto F, Nishida E. Nuclear translocation of plk1 mediated by its bipartite nuclear localization signal. *J. Biol. Chem*. 2002; 277:48884–48888. [PubMed: 12364337]
 60. Mehta TS, Lu H, Wang X, Urvalek AM, Nguyen KH, Monzur F, Hammond JD, Ma JQ, Zhao J. A unique sequence in the N-terminal regulatory region controls the nuclear localization of KLF8 by cooperating with the C-terminal zinc-fingers. *Cell Res*. 2009; 19:1098–1109. [PubMed: 19488069]
 61. LaCasse EC, Lefebvre YA. Nuclear localization signals overlap DNA- or RNA-binding domains in nucleic acid-binding proteins. *Nucleic Acids Res*. 1995; 23:1647–1656. [PubMed: 7540284]
 62. Skowrya D, Craig KL, Tyers M, Elledge SJ, Harper JW. F-box proteins are receptors that recruit phosphorylated substrates to the SCF ubiquitin-ligase complex. *Cell*. 1997; 91:209–219. [PubMed: 9346238]
 63. Kong YC, Morris GP, Brown NK, Yan Y, Flynn JC, David CS. Autoimmune thyroiditis: a model uniquely suited to probe regulatory T cell function. *J. Autoimmun*. 2009; 33:239–246. [PubMed: 19822405]

64. Yang L, Anderson DE, Baecher-Allan C, Hastings WD, Bettelli E, Oukka M, Kuchroo VK, Hafler DA. IL-21 and TGF-beta are required for differentiation of human T(H)17 cells. *Nature*. 2008; 454:350–352. [PubMed: 18469800]
65. Manel N, Unutmaz D, Littman DR. The differentiation of human T (H)-17 cells requires transforming growth factor-beta and induction of the nuclear receptor RORgamma. *Nat. Immunol.* 2008; 9:641–649. [PubMed: 18454151]
66. Numasaki M, Fukushi J, Ono M, Narula SK, Zavodny PJ, Kudo T, Robbins PD, Tahara H, Lotze MT. Interleukin-17 promotes angiogenesis and tumor growth. *Blood*. 2003; 101:2620–2627. [PubMed: 12411307]

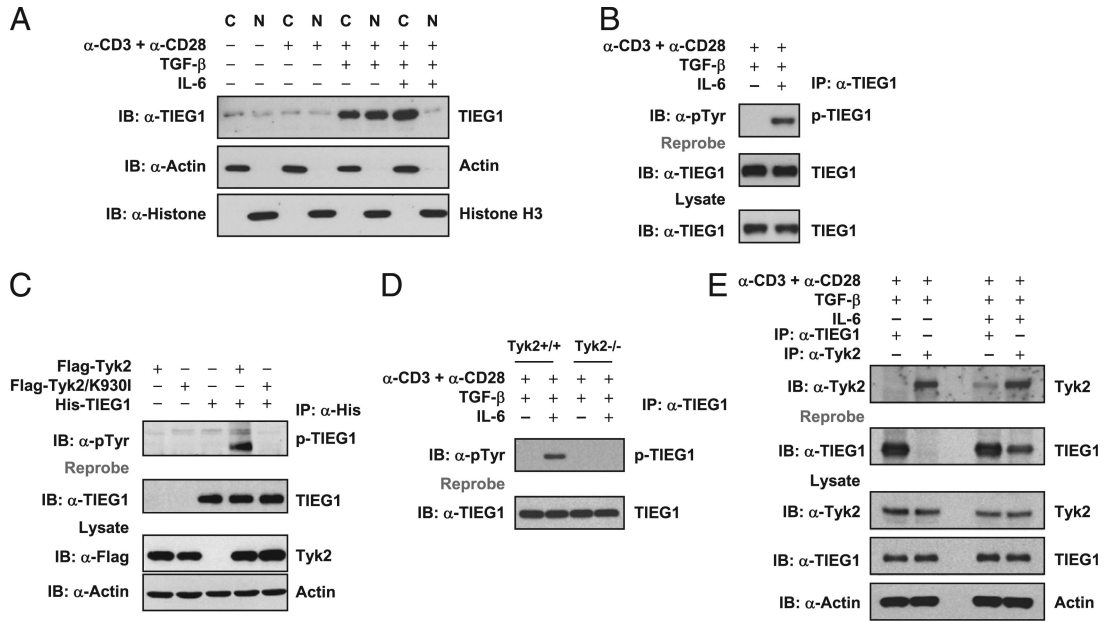


FIGURE 1.

IL-6–Tyk2 pathway-mediated phosphorylation regulates TIEG1 nuclear localization and Treg/Th17 differentiation. **A**, Naive CD4⁺CD25⁻ T cells were stimulated with anti-CD3 and anti-CD28 in the presence of TGF-β (5 ng/ml) alone or TGF-β (5 ng/ml) plus IL-6 (20 ng/ml). The nuclear and cytoplasmic fractions were immunoblotted with anti-TIEG1 Ab. The membranes were reprobated with anti-histone H3 and anti-actin Ab. C, cytoplasmic; N, nuclear. **B**, CD4⁺CD25⁻ T cells were treated as in **A**. Endogenous TIEG1 from total-cell lysates was immunoprecipitated with anti-TIEG1 Ab and immunoblotted with anti-phosphotyrosine Ab. Blots were reprobated using anti-TIEG1 Ab, p-TIEG1, or tyrosine-phosphorylated TIEG1. **C**, 293T cells were transfected with plasmids encoding His-TIEG1, Flag-Tyk2, or Flag-Tyk2/K930I, alone or in combination, for 24 h. TIEG1 was immunoprecipitated with anti-His Ab and immunoblotted with anti-phos-tyrosine Ab. Blot was stripped and reprobated with anti-TIEG1. The amount of Tyk2 in total-cell lysates was determined by immunoblotting. Actin was used as an equal loading control. **D**, Naive CD4⁺CD25⁻ T cells isolated from Tyk2^{+/+} and Tyk2^{-/-} mice were stimulated with anti-CD3 and anti-CD28 in the presence of TGF-β (5 ng/ml) alone or TGF-β (5 ng/ml) plus IL-6 (20 ng/ml). TIEG1 was immunoprecipitated using anti-TIEG1 Ab and immunoblotted using anti-phos-tyrosine Ab. **E**, TIEG1 interacts with Tyk2 in primary CD4 T cells. CD4⁺CD25⁻ T cells were stimulated with TGF-β or TGF-β plus IL-6, as described above. Endogenous TIEG1 or Tyk2 was immunoprecipitated with corresponding Abs and analyzed by immunoblotting with anti-Tyk2. The same blot was stripped and reprobated with anti-TIEG1. The amount of TIEG1 and Tyk2 in total-cell extracts was determined by Western blotting. Actin was used as an equal loading control.

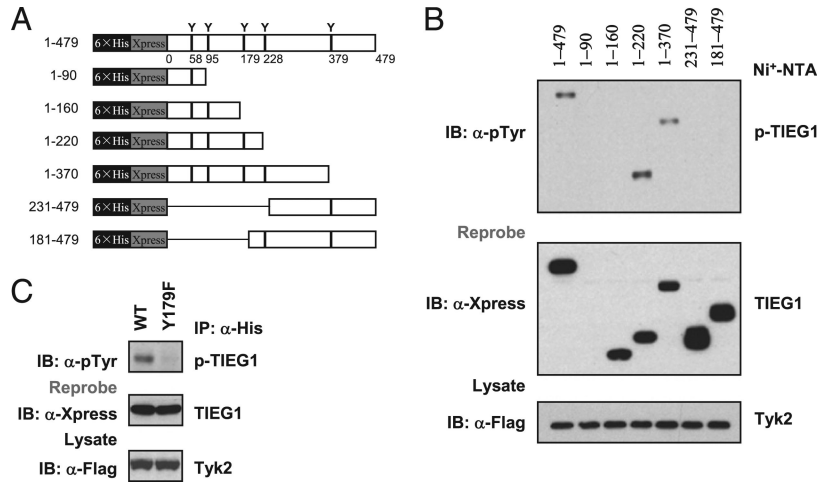


FIGURE 2. Tyk2 phosphorylates TIEG1 at Tyr179. *A*, Truncated mutants of TIEG1. Each tyrosine residue in individual truncated mutants is indicated. 6×His and Xpress represent His₆ tag and Xpress tag, respectively. *B*, 293T cells were cotransfected with plasmids encoding Flag-Tyk2 and truncated TIEG1 for 24 h. TIEG1 was precipitated by Ni-NTA affinity purification and immunoblotted with anti-phosphotyrosine Ab (*upper panel*). The same blot was stripped and reprobbed with anti-Xpress (*middle panel*). *C*, 293T cells were cotransfected with plasmids encoding Flag-Tyk2 and TIEG1 or TIEG1/Y179F mutant for 24 h. TIEG1 was immunoprecipitated with anti-His Ab and analyzed by immunoblotting with anti-phosphotyrosine Ab. The results shown are from one representative experiment that was conducted three times.

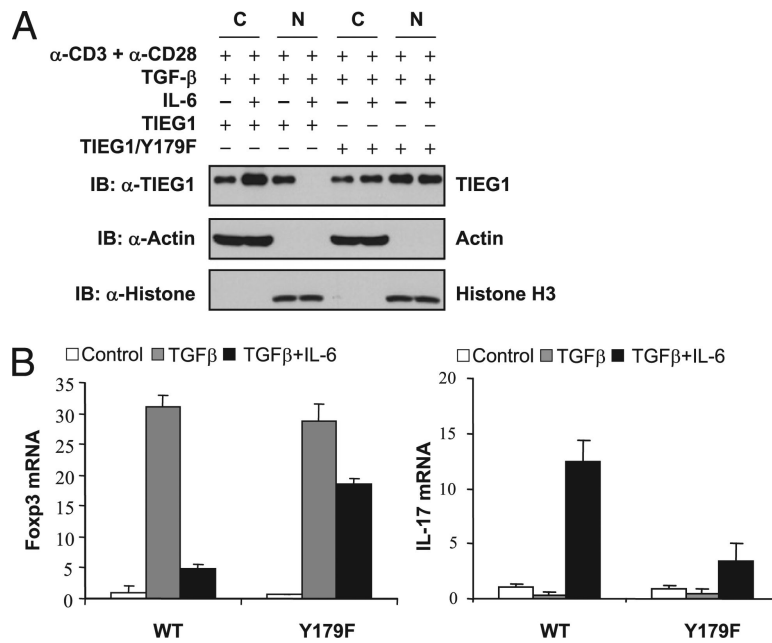


FIGURE 3. Tyk2-mediated phosphorylation regulates TIEG1 nuclear localization and Treg/Th17 differentiation. *A*, Naive TIEG1^{-/-} CD4⁺ CD25⁻ cells were reconstituted with WT or TIEG1-Y179F mutant by retroviral transduction. Nuclear/cytoplasmic localization of TIEG1 was analyzed in FACS-sorted GFP⁺ cells following treatment with TGF- β or TGF- β + IL-6. *B*, GFP⁺ cells were stimulated with TGF- β (Treg-inducing) and TGF- β + IL-6 (Th17-inducing) conditions for 7 d. The effect of Y179F mutation on Foxp3 versus IL-17 expression was analyzed by real-time PCR. The results shown are from one representative experiment that was conducted three times.

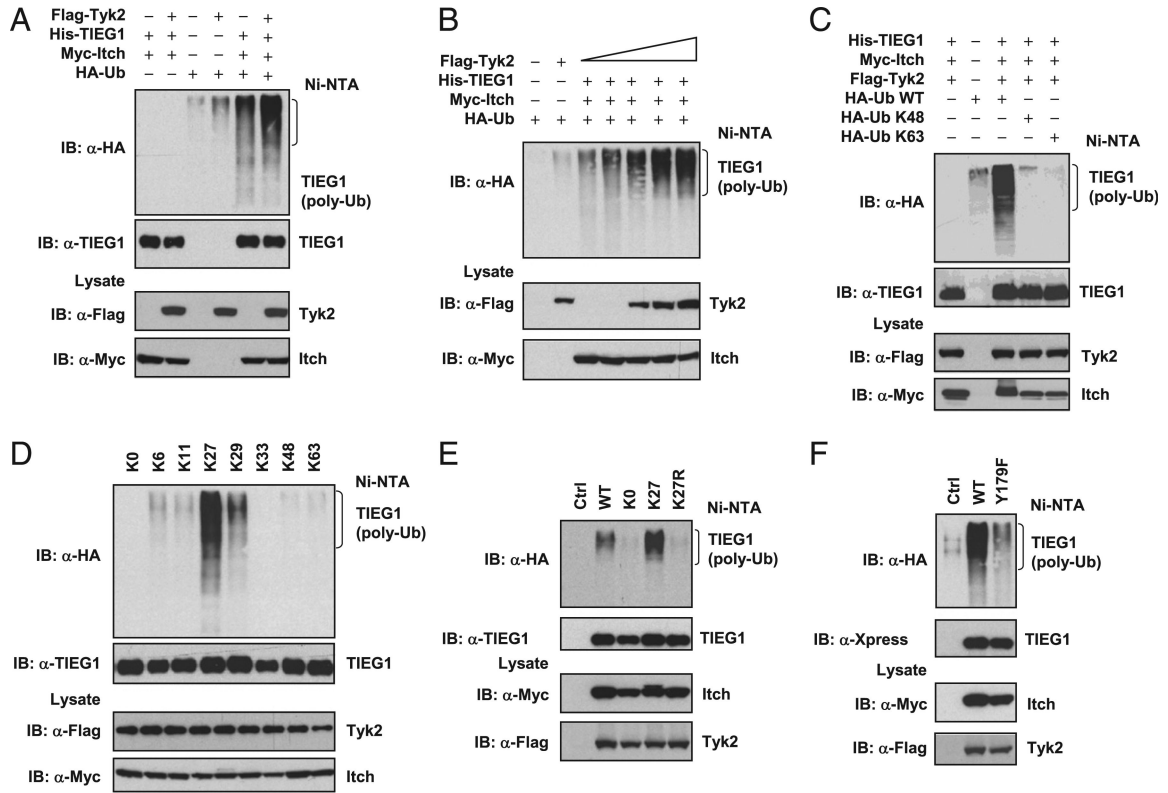
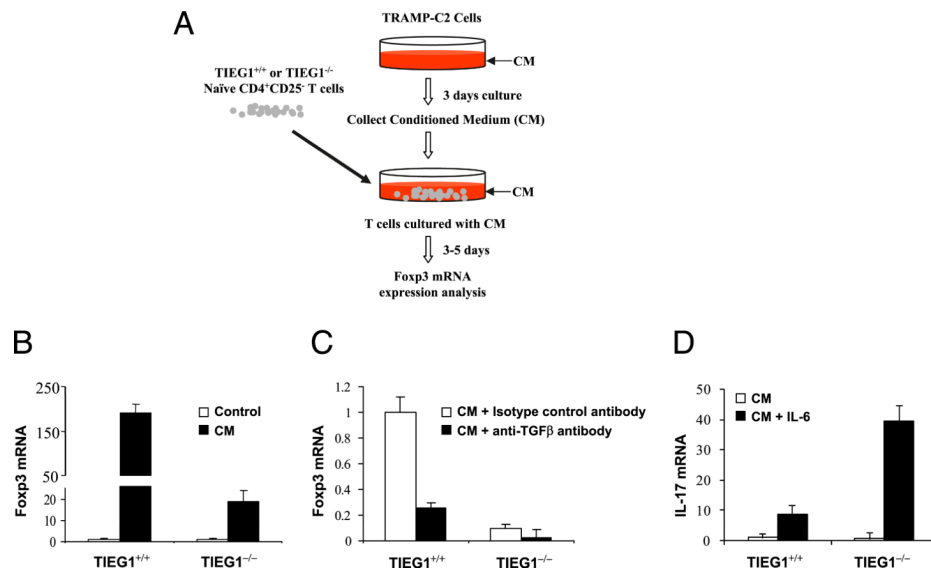


FIGURE 4. Tyk2-mediated phosphorylation-dependent polyubiquitination of TIEG1 is K27 linked. *A*, 293T cells were transfected with the indicated combination of plasmids encoding Flag-Tyk2, His-TIEG1, Myc-Itch, and HA-Ub for 48 h. Ubiquitinated TIEG1 was purified by Ni-NTA precipitation and analyzed by immunoblotting with anti-HA Ab. The expression of Tyk2 and Itch from total-cell lysates is shown (*bottom two panels*). *B*, 293T cells were transfected with plasmids encoding His-TIEG1, Myc-Itch, HA-Ub, and increased amounts of Flag-Tyk2. The ubiquitinated TIEG1 was purified by Ni-NTA precipitation and analyzed by immunoblotting with anti-HA Ab. *C*, 293T cells were transfected with plasmids encoding His-TIEG1, Myc-Itch, Flag-Tyk2, and HA-Ub or Ub-K48 or Ub-K63 (Ub-K48, only lysine K48 present, all other lysine mutated into arginine; Ub-K63, only lysine K63 present, all others mutated into arginine) for 40 h. Ubiquitinated TIEG1 was precipitated by Ni-NTA beads and analyzed by Western blotting with anti-HA Ab. The same blot was stripped and reprobed with anti-TIEG1. *D*, 293T cells were transfected with plasmids encoding His-TIEG1, Myc-Itch, Flag-Tyk2, and various lysine mutants of HA-ubiquitin (K0, all lysines are mutated into arginine; K6, K11, K27, K29, K33, K48, and K63, a single lysine present, all other lysines mutated into arginine). Ubiquitinated TIEG1 was precipitated and blotted with anti-HA Ab. *E*, 293T cells were transfected with Flag-Tyk2, Myc-Itch, and His-TIEG1 and HA-Ub WT, K0, K27, or K27R (K27R, only lysine K27 mutated into arginine, all other lysines present). The polyubiquitination of TIEG1 was determined by immunoblotting with anti-HA. *F*, 293T cells were transfected with Flag-Tyk2, Myc-Itch, HA-UbK27, His-TIEG1 WT, or His-TIEG1/Y179F mutant in 293T cells. The polyubiquitination of TIEG1 was determined by immunoblotting with anti-HA. The results shown are from one representative experiment that was conducted three times.

**FIGURE 5.**

Defective TGF- β induced Treg development in TIEG1^{-/-} naive CD4 T cells. *A*, Experimental procedures. TRAMP-C2 cells were cultured for 3 d without change of the medium. CM was collected and incubated with naive CD4⁺CD25⁻ T cells isolated from spleen and lymph nodes of TIEG1^{+/+} and TIEG1^{-/-} mice in the presence of anti-CD3 and anti-CD28. After 3–5 d of culture with CM, T cells were harvested for Foxp3 analysis. *B*, Real-time PCR analysis of Foxp3 expression. CD4⁺CD25⁻ T cells were stimulated with or without CM as in *A*, and Foxp3 expression level was analyzed by real-time PCR. The increased folds of Foxp3 mRNA were normalized to that of actin mRNA. *C*, In a similar experiment to *B*, anti-TGF- β (15 μ g/ml) or control isotype Ab was added to the cultures. Foxp3 mRNA was analyzed by real-time PCR. *D*, In a similar experiment to *A*, IL-6 was added to the T cell cultures. IL-17 mRNA was analyzed by real-time PCR.

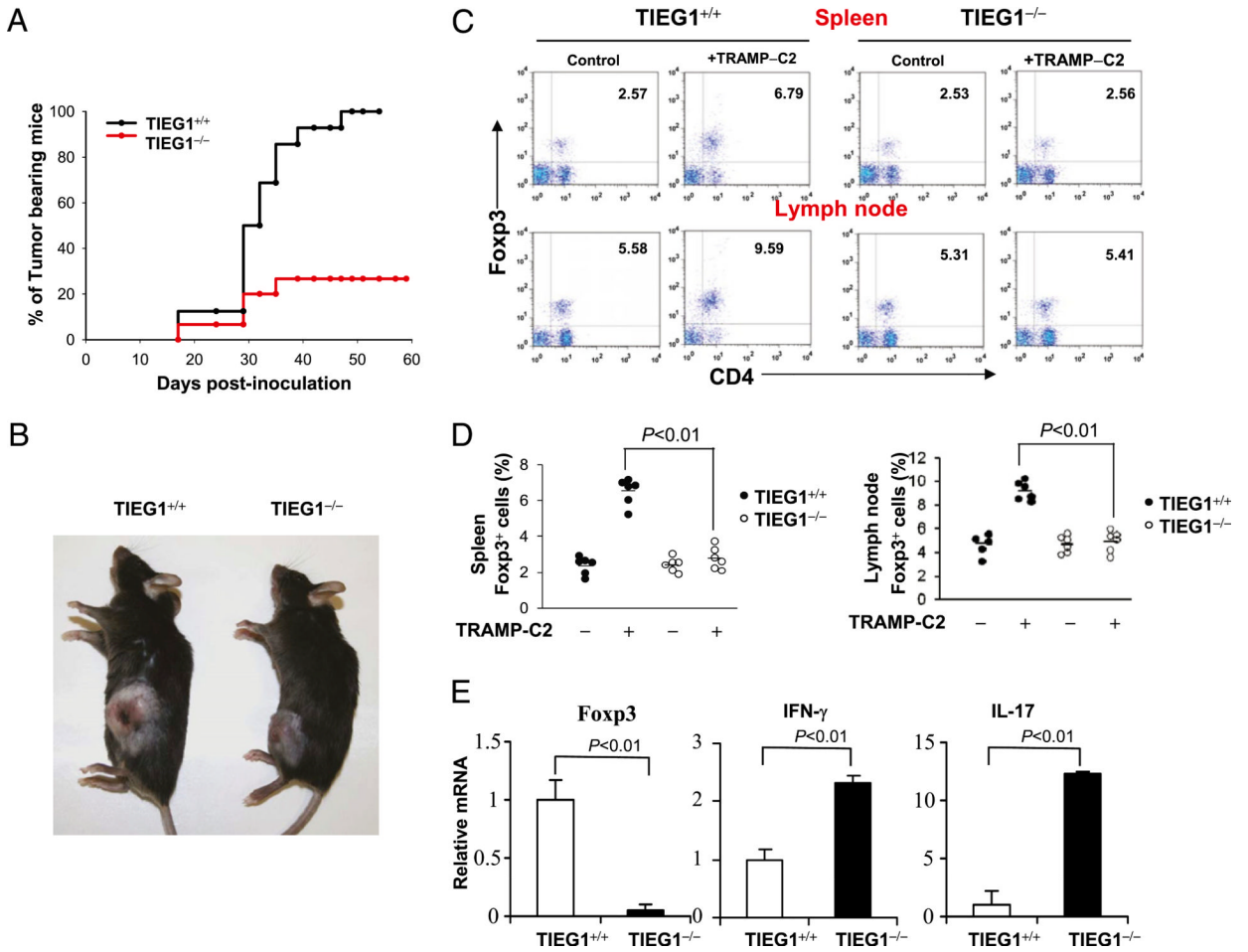


FIGURE 6. Elevated antitumor immune response in TIEG1^{-/-} mice. *A*, Kaplan–Meier curves of tumor-bearing TIEG1^{+/+} mice ($n = 16$) and TIEG1^{-/-} mice ($n = 16$). Male mice were injected s.c. with TRAMP-C2 cells. Tumors were monitored three times per week. Tumor incidence in each group was calculated from days 17–60. *B*, Representative image of tumor-bearing TIEG1^{+/+} and TIEG1^{-/-} mice. The photograph was taken at day 60 after initial inoculation. *C*, Fopx3⁺ Tregs in the spleen (*upper panels*) and lymph nodes (*lower panels*) from tumor-bearing (+TRAMP-C2) or control mice (–TRAMP-C2) were analyzed using FACS following intracellular staining using anti-Fopx3 Ab. *D*, CD4⁺Fopx3⁺ cell numbers in the spleen and lymph nodes of TIEG1^{+/+} and TIEG1^{-/-} mice. Each symbol represents an individual mouse. *E*, Tumor tissues were collected from TIEG1^{+/+} mice or TIEG1^{-/-} mice, and Fopx3, IFN-γ, and IL-17 expression was analyzed by real-time PCR. The results shown are from one representative experiment that was conducted three times.

NIH-PA Author Manuscript

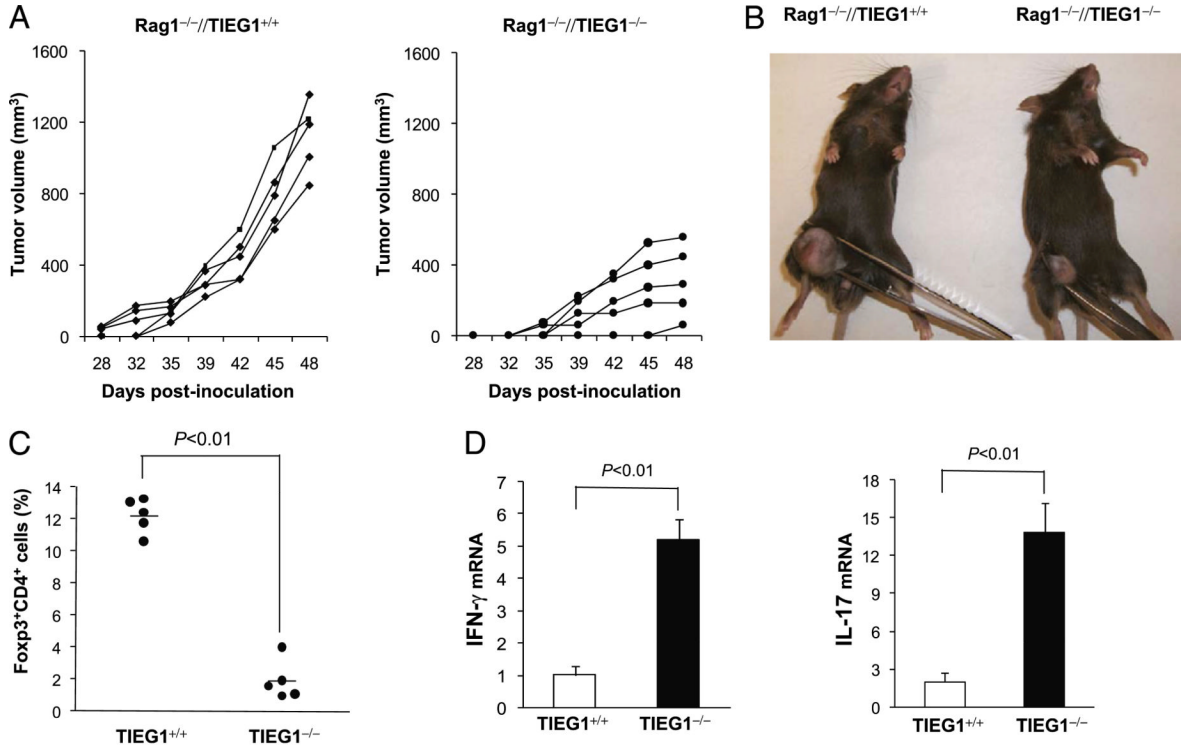


FIGURE 7. Adoptive transfer of TIEG1-deficient T cells inhibits TRAMP-C2 tumor growth. Rag1^{-/-} mice were injected s.c. with TRAMP-C2 cells on day 0. On day 3, naive CD4⁺CD25⁻ (3×10^6) and CD8⁺ T cells (3×10^6) from TIEG1^{+/+} and TIEG1^{-/-} mice were adoptively transferred (i.v.) into these Rag1^{-/-} mice ($n = 5$). **A**, The kinetics of tumor growth. **B**, Representative image of tumor-bearing Rag1^{-/-} mice. **C**, Percentage of CD4⁺Foxp3⁺ cells in tumor-infiltrated cells. **D**, Relative mRNA levels of IFN- γ and IL-17 in tumor-infiltrated lymphocytes.